Journal of Alloys and Compounds 513 (2012) 86–90

Contents lists available at SciVerse ScienceDirect

Journal of Alloys and Compounds

journal homepage: www.elsevier.com/locate/jallcom

$MSi_2O_{2-\delta}N_{2+2/3\delta}$:Eu (M = Sr, Ba) phosphors for field emission displays

Yanhua Song[a], Xuechun Xu[b], Haifeng Zou[a,*], Ye Sheng[a], Hongpeng You[c,*]

[a] College of Chemistry, Jilin University, Changchun 130026, PR China
[b] College of Earth Sciences, Jilin University, Changchun 130061, PR China
[c] State Key Laboratory of Rare Earth Resource Utilization, Changchun Institute of Applied Chemistry, Chinese Academy of Sciences, Changchun 130022, PR China

ARTICLE INFO

Article history:
Received 27 April 2011
Received in revised form
28 September 2011
Accepted 30 September 2011
Available online 18 October 2011

Keywords:
Oxynitride
Field emission displays
Green phosphor
Cyan phosphor

ABSTRACT

$MSi_2O_{2-\delta}N_{2+2/3\delta}$:$Eu^{2+}$ (M = Sr, Ba) phosphors were prepared through a two-step solid state reaction. XRD results reveal that the samples are nitrogen-rich phase. The photoluminescence results show that the $MSi_2O_{2-\delta}N_{2+2/3\delta}$:Eu (M = Sr, Ba) phosphors can be excited by UV and blue light. The critical concentrations of Eu^{2+} are 5 mol% and 4 mol% for $MSi_2O_{2-\delta}N_{2+2/3\delta}$:Eu (M = Sr, Ba), respectively. With an increase of the Eu^{2+}-concentration, the emission color of $SrSi_2O_{2-\delta}N_{2+2/3\delta}$:Eu can be tuned from green to yellow. Under the excitation of low voltage electron beams (1–3 kV), the $MSi_2O_{2-\delta}N_{2+2/3\delta}$:Eu (M = Sr, Ba) phosphors exhibit green and cyan emission, respectively. The emission intensity increases with the increasing of accelerating voltage and filament current. Due to the excellent stability, good CIE chromaticity and high color purity, $MSi_2O_{2-\delta}N_{2+2/3\delta}$:Eu (M = Sr, Ba) phosphors may have potential application in the field emission displays.

1. Introduction

Field emission displays (FEDs) have been considered as promising candidates for next generation display due to their certain specific advantages, such as low power consumption, wide viewing angle, better compactness, low weight to size ratio and high resolution, etc. [1]. FEDs must operate at low voltage (<5 kV) and high current density. So the phosphors used in FEDs are required to have high efficiency at low voltages, high resistance to current saturation, long service time, and good chromaticity [2–4]. Many sulfide and oxide phosphors, such as, ZnS:Cu,Au,Al, $SrGa_2S_4$:Eu^{3+}, and Y_2O_3:Eu^{3+}, have been explored as possible low-voltage excited phosphors. However, sulfide-based phosphors are chemical instable during operation and the emitter cathode in FEDs could be eroded by sulfur related contaminant gases and the device lifetime would be shortened [5]. Although oxide phosphors are more stable than the sulfides, they are usually insulators. When they are excited by low-voltage electron beam with high current density, a lot of electrons are accumulated on the phosphor's surface due to the poor conductivity of the oxide phosphors, resulting in the decrease of the phosphor luminance and luminous efficiency [6]. Therefore, it is necessary to find novel phosphors with high luminescence efficiency, good stability and reasonable conductivity in order to improve the performance of FED devices.

Oxynitride/nitride-based phosphors with excellent chemical and thermal stabilities show outstanding luminescence properties, such as good quantum efficiency, radiation stability, and excellent thermal quenching behavior [7]. They are promising candidates for white light-emitting diodes (LEDs). Representative candidates are $Sr_2Si_5N_8$:Eu^{2+} (red) [8,9], $CaAlSiN_3$:Ce^{3+} [10,11], Ca-α-Sialon:Eu^{2+} ($Ca_{(m/2)-x}Eu_xSi_{12-m-n}Al_{m+n}O_nN_{16-n}$) [12], β-Sialon:$Eu^{2+}$ ($Si_{6-z}Al_zO_zN_{8-z}$, $0 < z \leq 4.2$) [13], $MSi_2O_{2-\delta}N_{2+2/3\delta}$ (M = Ca, Sr, Ba):Eu^{2+} [14], and Sr-Sialon:Eu^{2+}(blue to yellow) [15]. Among these phosphors, $MSi_2O_{2-\delta}N_{2+2/3\delta}$ (M = Ca, Sr, Ba):Eu^{2+} was reported to have efficient cyan or green emission. The existence of N in the formula will lower the gravity center, so the excited state of the 5d level of Eu^{2+} ions will be lowered significantly due to large crystal-field splitting and strong nephelauxetic effect [16]. So the emission color of $MSi_2O_{2-\delta}N_{2+2/3\delta}$ (M = Ca, Sr, Ba):Eu^{2+} can be tuned by the account of N or the content of Eu^{2+} ions. Although their photoluminescence properties have been widely investigated, the cathodoluminescence was rarely reported. In this paper, we synthesized $MSi_2O_{2-\delta}N_{2+2/3\delta}$ (M = Sr, Ba):Eu^{2+} with different Eu^{2+} contents by two-step solid state reaction method. Their Eu^{2+} concentrations related photoluminescent properties and the low voltage cathodoluminescent properties are investigated.

2. Experimental

2.1. Preparation

All powder samples of $MSi_2O_{2-\delta}N_{2+2/3\delta}$:$Eu^{2+}$(M = Sr, Ba) were synthesized by a two-step high-temperature solid state reaction. The starting materials were MCO_3 (M = Sr, Ba) (A.R.), β-Si_3N_4 (99%), and Eu_2O_3 (99.99%). The Eu^{2+} mole fractions with

* Corresponding authors.
E-mail addresses: zouhf@jlu.edu.cn (H. Zou), hpyou@ciac.jl.cn (H. You).

0925-8388/$ – see front matter. Crown Copyright © 2011 Published by Elsevier B.V. All rights reserved.
doi:10.1016/j.jallcom.2011.09.090

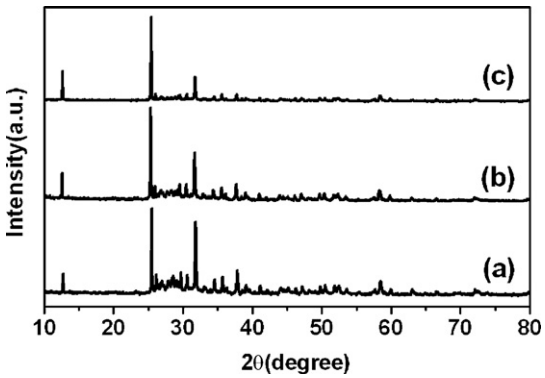

Fig. 1. XRD patterns of $Sr_{1-x}Eu_xSi_2O_{2-\delta}N_{2+2/3\delta}$ with different Eu concentration. (a) $SrSi_2O_{2-\delta}N_{2+2/3\delta}$; (b) $Sr_{0.99}Eu_{0.01}Si_2O_{2-\delta}N_{2+2/3\delta}$; (c) $Sr_{0.50}Eu_{0.50}Si_2O_{2-\delta}N_{2+2/3\delta}$.

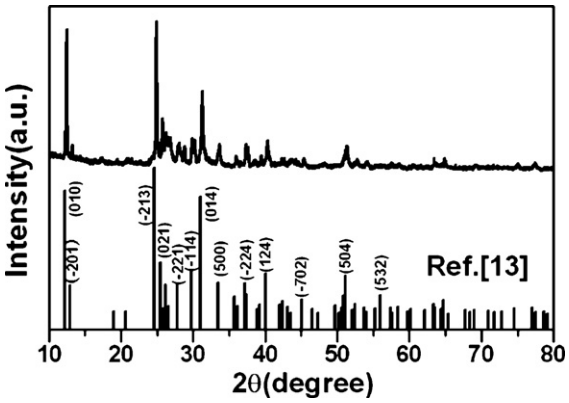

Fig. 2. XRD patterns of $Ba_{0.95}Eu_{0.05}Si_2O_{2-\delta}N_{2+2/3\delta}$ as well as the data reported by Ref. [17] as a reference.

respect to the M^{2+} ion range from 1% to 50%. Stoichiometric amount of raw materials were thoroughly mixed by grinding in an agate mortar. Subsequently, the mixtures were transferred into crucibles and preheated at 1200 °C for 2 h to decompose the $SrCO_3$ (or $BaCO_3$) and then the temperature was increased to 1500 °C and maintained for 3 h to obtain the final product. The firing was carried out in a N_2 atmosphere.

2.2. Characterizations

Powder X-ray diffraction (XRD) measurements were performed on a Bruker D8 focus X-ray powder diffractometer with Cu Kα radiation (λ = 0.15405 nm). Photoluminescence (PL) excitation and emission spectra were recorded with a Hitachi F-4500 spectrophotometer equipped with a 150 W xenon lamp as the excitation source. The cathodoluminescent measurements were carried out in an ultrahigh-vacuum chamber (<10^{-8} Torr), where the samples were excited by an electron beam at a voltage range of 1–3 kV with different filament currents, and the spectra were recorded on an F-4500 spectrophotometer. The luminescence decay curves were obtained from a Lecroy Wave Runner 6100 Digital Osilloscope (1 GHz) using a tunable laser (pulse width = 4 ns, gate = 50 ns) as the excitation (Continuum Sunlite OPO). All the measurements were performed at room temperature.

3. Results and discussion

3.1. Crystal structure

Fig. 1 shows the XRD patterns of $Sr_{1-x}Eu_xSi_2O_{2-\delta}N_{2+2/3\delta}$ with different Eu^{2+} contents. All the patterns can be well indexed to a $SrSi_2O_{2-\delta}N_{2+2/3\delta}$ phase comparing with literature [14]. When the strongest peak is at about $2\theta \approx 25.43^\circ$, it means that the sample is nitrogen-rich $SrSi_2O_{2-\delta}N_{2+2/3\delta}$ ($\delta \approx 1$). When the strongest peak is at about $2\theta \approx 31.78^\circ$, the sample is oxygen-rich $SrSi_2O_{2-\delta}N_{2+2/3\delta}$ ($\delta \approx 0$) [14]. With the increasing of Eu content, the peak at about $2\theta \approx 25.43^\circ$ becomes stronger than that at about $2\theta \approx 31.78^\circ$, indicating that the as-obtained samples tend to be nitrogen-rich phase $SrSi_2O_{2-\delta}N_{2+2/3\delta}$ ($\delta \approx 1$). The energy-dispersive X-ray spectrum (EDX) analysis shows that the element ratios of Sr, Si, O, N, and Eu are 12.91/24.14/24.52/25.38/0, 13.87/27.18/27.64/28.69/0.18, and 6.71/22.46/26.58/34.47/4.86 for $SrSi_2O_{2-\delta}N_{2+2/3\delta}$, $Sr_{0.99}Eu_{0.01}Si_2O_{2-\delta}N_{2+2/3\delta}$, and $Sr_{0.50}Eu_{0.50}Si_2O_{2-\delta}N_{2+2/3\delta}$, respectively. The EDX results conform that the N content in the formula increases as the increasing of Eu content. Fig. 2 shows the XRD pattern of $BaSi_2O_{2-\delta}N_{2+2/3\delta}$. It matches well with that reported in the literature [17].

3.2. Photoluminescence properties

Fig. 3(A) shows the normalized excitation spectra of $Sr_{1-x}Eu_xSi_2O_{2-\delta}N_{2+2/3\delta}$ with different Eu^{2+} concentration. For all the samples, the excitation curves are composed of one broad band from 200 to 500 nm, which can be ascribed to the host absorption and the $4f^7 \rightarrow 4f^6 5d$ transition of the Eu^{2+} ion. With the increasing of Eu^{2+} concentration, the excitation band becomes broader and the strongest peak moves from 380 to 473 nm. The intensity enhancement in the visible range of 400–460 nm makes the phosphors match well with the emission of the blue-InGaN based LEDs. The emission spectra for $Sr_{1-x}Eu_xSi_2O_{2-\delta}N_{2+2/3\delta}$ excited at 450 nm are presented in Fig. 3(B). A broad band emission peak can be observed and ascribed to the $4f^6 5d \rightarrow 4f^7$ transition of the Eu^{2+} ions. With the increase of Eu^{2+} concentration from $x = 0.01$ to $x = 0.50$, the emission maximum shifts from 532 to 550 nm. Corresponding emission color can be tuned from green to yellow. The red-shift in excitation and emission spectra may be mainly ascribed to the following two reasons. According to the XRD results,

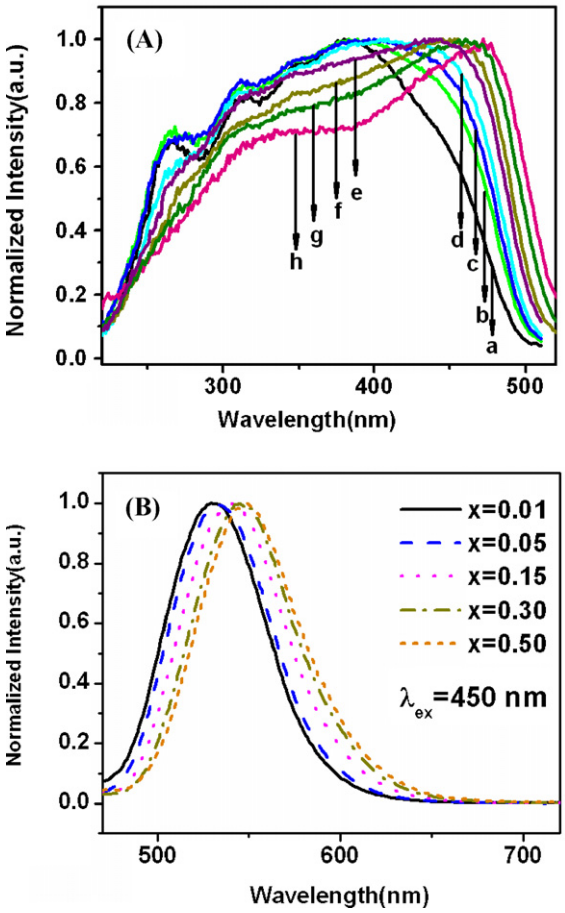

Fig. 3. Normalized excitation (A) and emission (B) spectra for $Sr_{1-x}Eu_xSi_2O_{2-\delta}N_{2+2/3\delta}$ with different Eu concentration. (a): $x = 0.01$; (b): $x = 0.03$; (c): $x = 0.04$; (d): $x = 0.05$; (e): $x = 0.10$; (f): $x = 0.15$; (g): $x = 0.30$; (h): $x = 0.50$.

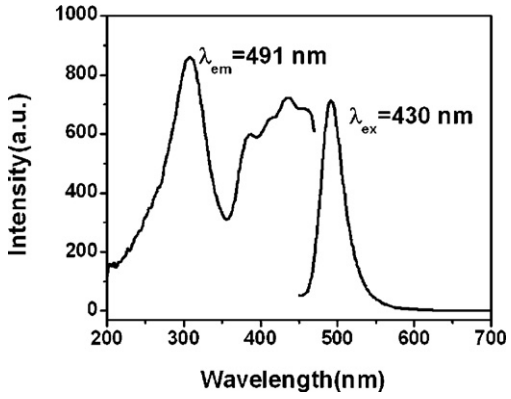

Fig. 4. Excitation and emission spectra for $Ba_{0.95}Eu_{0.05}Si_2O_{2-\delta}N_{2+2/3\delta}$.

the samples tend to form nitrogen-rich phase $SrSi_2O_{2-\delta}N_{2+2/3\delta}$ ($\delta \approx 1$) at higher Eu^{2+} concentration. Compared with O^{2-}, N^{3-} has higher formal charge and lower electronegativity. So the ligand-field splitting of the 5d levels of Eu^{2+} ions in nitrogen-rich surrounding becomes larger and the center of gravity of the 5d states shifts to lower energy [18]. The other reason is the changes in the crystal field around Eu^{2+} ions, which results from the slight distortion of the crystal structure [19].

Fig. 4 shows the excitation and emission spectra of $Ba_{0.95}Eu_{0.05}Si_2O_{2-\delta}N_{2+2/3\delta}$. The excitation spectrum has two broad bands in the range of 200 to 450 nm, which are ascribed to the host absorption and the $4f^7 \rightarrow 4f^65d$ transition of the Eu^{2+} ions. Under the excitation of 430 nm, $Ba_{0.95}Eu_{0.05}Si_2O_{2-\delta}N_{2+2/3\delta}$ exhibits cyan emission with maximum peak at 491 nm. The PL properties are similar to that reported by Li et al. [14]. All the excitation spectra are composed of broad band from 200 to 500 nm. But the emission spectra have a little difference. In the literature reported by Li, the main position of the emission peaks for $Sr_{0.9}Eu_{0.1}Si_2O_2N_{2+2/3\delta}$:$Eu^{2+}$ and $Ba_{0.9}Eu_{0.1}Si_2O_2N_{2+2/3\delta}$:$Eu^{2+}$ are located at much longer wavelength (570 and 500 nm). This difference may be ascribed to two reasons. One is that the exact content of nitrogen in the formula may be different. The other one is that the optical measurement conditions are different.

The dependencies of emission intensity of $M_{1-x}Eu_xSi_2O_{2-\delta}N_{2+2/3\delta}$ (M = Sr, Ba) on the Eu^{2+} concentration are shown in Fig. 5. The concentration quenching occurs when the Eu^{2+} concentrations are 5 mol% and 4 mol% for $Sr_{1-x}Eu_xSi_2O_{2-\delta}N_{2+2/3\delta}$ and $Ba_{1-x}Eu_xSi_2O_{2-\delta}N_{2+2/3\delta}$, respectively. The fluorescent mechanism of the Eu^{2+} ions in $M_{1-x}Eu_xSi_2O_{2-\delta}N_{2+2/3\delta}$ (M = Sr, Ba) phosphor is the 5d–4f allowed electric-dipole transition, so the process of the energy transfer should be controlled by electric multipole–multipole interaction according to Dexter's theory [10]. If the energy transfer occurs between the same sorts of activators, the intensity of multipolar interaction can be determined from the change of the emission intensity from the emitting level, which has the multipolar interaction. The emission intensity (I) per activator ion follows the equation [20,21]:

$$\frac{I}{x} = K[1 + \beta(\chi)^{Q/3}]^{-1} \quad (1)$$

where χ is the activator concentration; Q = 6, 8 or 10 represents dipole–dipole, dipole–quadrupole or quadrupole–quadrupole interaction, respectively; K and β are constants for the same excitation condition for a given host crystal. In order to obtain the value of Q, the curves of $\log(I/\chi_{Eu^{2+}})$ versus $\log(\chi_{Eu^{2+}})$ for $M_{1-x}Eu_xSi_2O_{2-\delta}N_{2+2/3\delta}$ (M = Sr, Ba) are presented in Fig. 6. Both of the plots are linear and the slopes are −1.81 and −2.29 for $M_{1-x}Eu_xSi_2O_{2-\delta}N_{2+2/3\delta}$ (M = Sr, Ba), respectively. The values of Q can be calculated to be 5.43 and 6.87 for $M_{1-x}Eu_xSi_2O_{2-\delta}N_{2+2/3\delta}$ (M = Sr, Ba), respectively. These results indicate that dipole–dipole interaction should be responsible for the concentration quenching of the Eu^{2+} ions in the $M_{1-x}Eu_xSi_2O_{2-\delta}N_{2+2/3\delta}$ (M = Sr, Ba) phosphors.

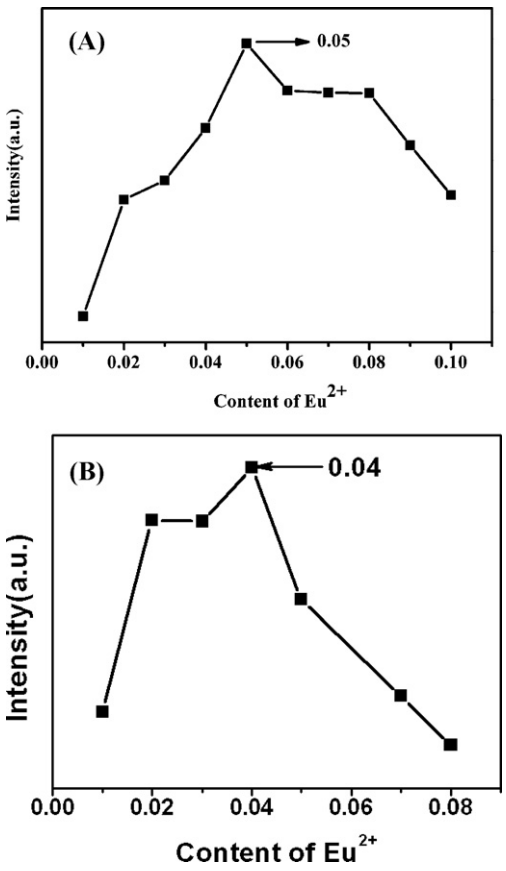

Fig. 5. PL intensities of $Sr_{1-x}Eu_xSi_2O_{2-\delta}N_{2+2/3\delta}$ (A) and $Ba_{1-x}Eu_xSi_2O_{2-\delta}N_{2+2/3\delta}$ (B) as a function of Eu^{2+} contents (x).

3.3. Cathodoluminescent properties

Under low-voltage electron beam excitation, the as prepared $MSi_2O_{2-\delta}N_{2+2/3\delta}$:Eu (M = Sr, Ba) phosphors exhibit green [the Commission International d'Eclairage (CIE) chromaticity coordinates are x = 0.28 and y = 0.57] and cyan (the CIE chromaticity coordinates are x = 0.14 and y = 0.35) emissions. The cyan emission of $BaSi_2O_{2-\delta}N_{2+2/3\delta}$:Eu can enlarge the color gamut of tricolor FEDs phosphors and thus increase the display quality of full-color FEDs [22]. The typical emission spectra of the $M_{0.95}Si_2O_{2-\delta}N_{2+2/3\delta}$:0.05Eu (M = Sr, Ba) under the excitation of electron beams (accelerating voltage = 3 kV) are shown in Fig. 7(a) and (b). Both of the emission spectra are identical with the photoluminescence spectra. The maximum peaks are located at 532 and 491 nm, which are attributed to the $4f^65d^1 \rightarrow 4f^7$ transition of Eu^{2+} ions. The full width at half maximum (FWHM) of the emission spectra for $MSi_2O_{2-\delta}N_{2+2/3\delta}$:Eu (M = Sr, Ba) phosphors are 68 and 39 nm, respectively. The narrow FWHM indicates that these two phosphors have high color purity which is highly propitious for application in the full-color FEDs. The CL emission intensities for $M_{0.95}Si_2O_{2-\delta}N_{2+2/3\delta}$:0.05Eu (M = Sr, Ba) phosphors have been investigated as a function of the accelerating voltage and the filament current, as shown in Fig. 8(a) and (b). When the filament current is fixed at 90 mA, the CL intensities increase with raising the accelerating voltage from 1 to 3 kV (Fig. 8(a)). Similarly, the CL intensities also increase with increasing the filament current

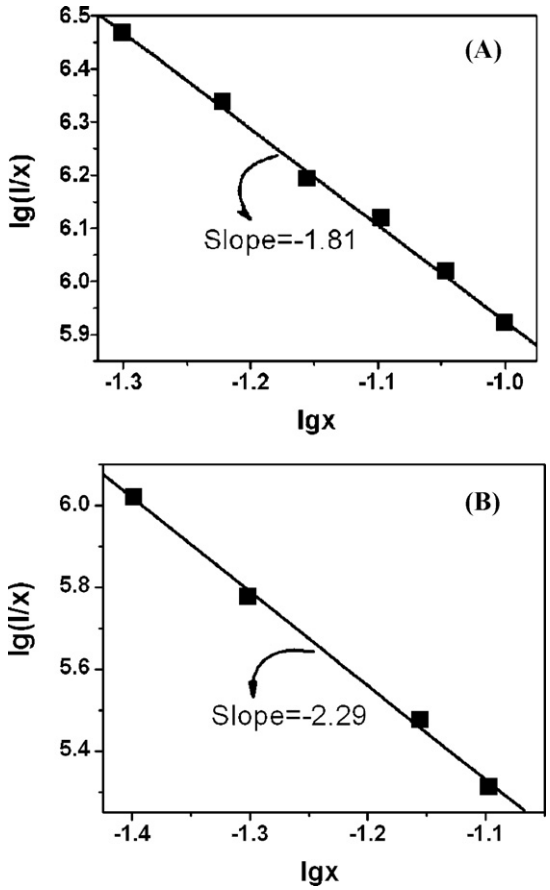

Fig. 6. The curves of $\log I/\chi_{Eu^{2+}}$ versus $\log \chi_{Eu^{2+}}$ for $Sr_{1-x}Eu_xSi_2O_{2-\delta}N_{2+2/3\delta}$ (A) and $Ba_{1-x}Eu_xSi_2O_{2-\delta}N_{2+2/3\delta}$ (B) phosphors.

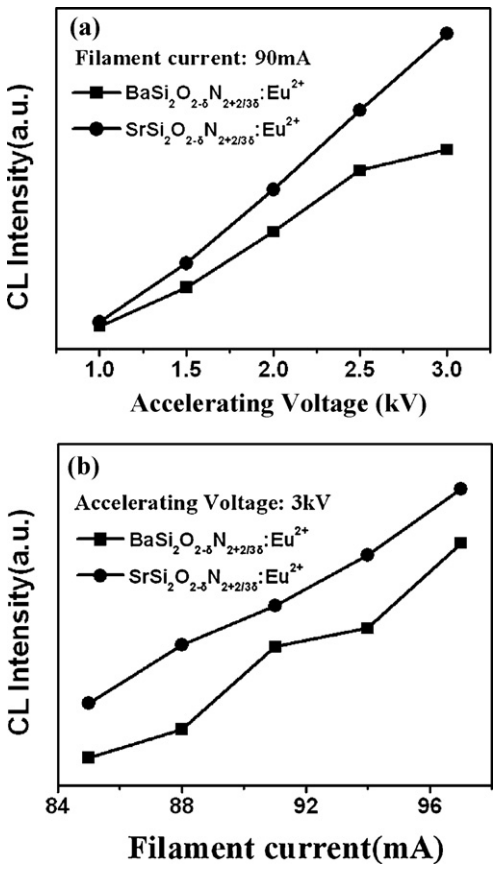

Fig. 8. The cathodoluminescence intensity of $Sr_{0.95}Eu_{0.05}Si_2O_{2-\delta}N_{2+2/3\delta}$ and $Ba_{0.95}Eu_{0.05}Si_2O_{2-\delta}N_{2+2/3\delta}$ samples as a function of accelerating voltage (a) and filament current (b).

from 85 to 97 mA when the accelerating voltage is fixed at 3 kV (Fig. 8(b)). The enhancement in CL intensity with an increase in electron energy can be attributed to the deeper penetration of the electrons into the phosphor body and the larger electron beam current density [23]. The electron penetration depth can be estimated using the empirical formula $L\,[\text{Å}] = 250(A/\rho)(E/Z^{1/2})^n$, where $n = 1.2/(1 - 0.29\log_{10} Z)$, A is the atomic or molecular weight of the material ρ is the bulk density, Z is the atomic number, and E is the accelerating voltage (kV) [24]. For $M_{0.95}Si_2O_{2-\delta}N_{2+2/3\delta}$:0.05Eu (M = Sr, Ba) phosphors, the Eu^{2+} ions are excited by the plasma produced by the incident electrons. With the increase of accelerating voltage or filament current, more plasma will be produced by the incident electrons, resulting in more populations of the excited Eu^{2+} ions and higher CL intensity [25].

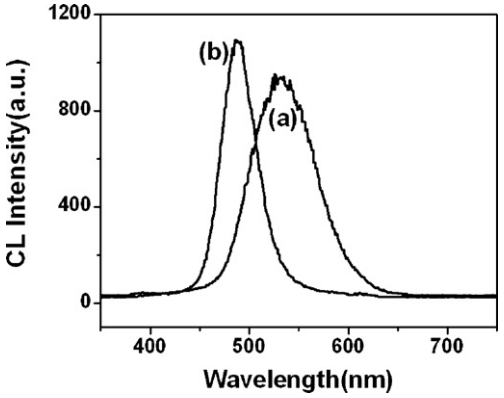

Fig. 7. Typical cathodoluminescence spectra of $Sr_{0.95}Eu_{0.05}Si_2O_{2-\delta}N_{2+2/3\delta}$ (a) and $Ba_{0.95}Eu_{0.05}Si_2O_{2-\delta}N_{2+2/3\delta}$ (b) (accelerating voltage: 3 kV; filament current: 90 mA).

4. Conclusions

In summary, Eu^{2+} doped $MSi_2O_{2-\delta}N_{2+2/3\delta}$ (M = Sr, Ba) green and cyan phosphors have been synthesized by solid state reaction. $MSi_2O_{2-\delta}N_{2+2/3\delta}$:$Eu^{2+}$(M = Sr, Ba) phosphors can effectively excited by UV or blue light. The critical quenching concentrations of Eu^{2+} are determined as 5 mol% and 4 mol% for $MSi_2O_{2-\delta}N_{2+2/3\delta}$:$Eu^{2+}$(M = Sr, Ba), respectively. The major mechanism for concentration quenching is dipole–dipole interaction. The emission color of $SrSi_2O_{2-\delta}N_{2+2/3\delta}$:$Eu^{2+}$ can be tuned from green to yellow by changing the Eu^{2+} concentration. Under the excitation of low voltage cathode rays, $MSi_2O_{2-\delta}N_{2+2/3\delta}$:$Eu^{2+}$(M = Sr, Ba) phosphors exhibit green and cyan emissions, respectively. The cathodoluminescence intensity of $MSi_2O_{2-\delta}N_{2+2/3\delta}$:$Eu^{2+}$ (M = Sr, Ba) phosphors increases with raising the accelerating voltage and filament current. The good stability and high color purity for $MSi_2O_{2-\delta}N_{2+2/3\delta}$:$Eu^{2+}$(M = Sr, Ba) phosphors make them have potential applications in FEDs area.

References

[1] X.G. Xu, J. Chen, S.Z. Deng, N.S. Xu, J. Lin, J. Vac. Sci. Technol. B 28 (2010) 490–494.
[2] G. Li, D. Geng, M. Shang, C. Peng, Z. Cheng, J. Lin, J. Mater. Chem. 21 (2011) 13334–13344.
[3] J. Liao, B. Qiu, H. Wen, J. Chen, W. You, L. Liu, J. Alloys Compd. 487 (2009) 758–762.
[4] X. Liu, J. Lin, Solid State Sci. 11 (2009) 2030–2036.
[5] G. Li, X. Xu, C. Peng, M. Shang, D. Geng, Z. Cheng, J. Chen, J. Lin, Opt. Express 19 (2011) 16423–16431.

[6] M. Shang, G. Li, D. Yang, X. Kang, C. Zhang, J. Lin, J. Electrochem. Soc. 158 (2011) J125–J131.
[7] Y. Song, N. Guo, H. You, Eur. J. Inorg. Chem. 14 (2011) 2327–2332.
[8] V.D. Luong, W. Zhang, H.R. Lee, J. Alloys Compd. 509 (2011) 7525–7528.
[9] M. Zeuner, P.J. Schmidt, W. Schnick, Chem. Mater. 21 (2009) 2467–2473.
[10] Y.Q. Li, N. Hirosaki, R.J. Xie, T. Takeda, M. Mitomo, Chem. Mater. 20 (2008) 6704–6714.
[11] B. Lei, K. Machida, T. Horikawa, H. Hanzawa, Chem. Lett. 39 (2010) 104–107.
[12] K. Shioi, N. Hirosaki, R.J. Xie, T. Takeda, Y.Q. Li, J. Alloys Compd. 504 (2010) 579–584.
[13] X.W. Zhu, Y. Masubuchi, T. Motohashi, S. Kikkawa, J. Alloys Compd. 489 (2010) 157–161.
[14] Y.Q. Li, A.C. Delsing, G.D. With, H.T. Hintzen, Chem. Mater. 17 (2005) 3242–3248.
[15] K. Shioi, Y. Michiue, N. Hirosaki, R.J. Xie, T. Takeda, Y. Matsushita, M. Tanaka, Y.Q. Li, J. Alloys Compd. 509 (2011) 332–337.
[16] R.-J. Xie, N. Hirosaki, Sci. Technol. Adv. Mater. 8 (2007) 588–600.
[17] Y.Q. Li, G. de With, H.T. Hintzen, J. Mater. Chem. 15 (2005) 4492–4496.
[18] R.-J. Xie, N. Hirosaki, M. Mitomo, Y. Yamamoto, T. Suehiro 1, J. Phys. Chem. B 108 (2004) 12027–12031.
[19] Z.C. Wu, J.X. Shi, J. Wang, M.L. Gong, Q. Su, J. Solid State Chem. 179 (2006) 2356–2360.
[20] L.G. Van Uitert, J. Electrochem. Soc. 114 (1967) 1048–1053.
[21] L. Ozawa, P.M. Jaffe, J. Electrochem. Soc. 118 (1971) 1678–1679.
[22] G. Li, X. Zhang, C. Peng, M. Shang, D. Geng, Z. Cheng, J. Lin, J. Mater. Chem. 21 (2011) 6477–6479.
[23] X. Liu, J. Lin, J. Appl. Phys. 100 (2006) 124306–124312.
[24] C. Feldman, Phys. Rev. 117 (1960) 455–457.
[25] G. Jia, Y. Song, M. Yang, K. Liu, Y. Zheng, H. You, J. Cryst. Growth 311 (2009) 4213–4218.